Advances in Marine Structures – Guedes Soares & Fricke (eds)
© 2011 Taylor & Francis Group, London, ISBN 978-0-415-67771-4

Numerical simulation of laterally impacted clamped circular steel plates

R. Villavicencio, L. Sutherland & C. Guedes Soares
Centre for Marine Technology and Engineering (CENTEC), Technical University of Lisbon, Instituto Superior Técnico, Lisboa, Portugal

ABSTRACT: The paper presents numerical simulations of previously reported drop weight impact tests examining the dynamic response of fully clamped steel circular plates struck transversely at the centre by a mass with a spherical indenter. The impact velocity varied from 0.5 to 6.0 m/s. The plates showed no visible damage at the very low incident energies, but suffered both permanent indentation and global deformation as incident energy was increased. The numerical modelling was performed using the LS-DYNA nonlinear, dynamic finite element software and is based on a previous finite element analysis of aluminium plates under lateral impact. The numerical calculations used can accurately predict the response of deflections, forces and absorbed energies, using both shell and solid element types. However, solid elements were required to obtain a satisfactorily accurate prediction of the deformed shape including the indentation into the thickness. The steel plastic response is compared and discussed with that of similar aluminium plates.

1 INTRODUCTION

The structural design of ships concerning collision requires an accurate prediction of the damage of stiffened plates under impact loading. Finite Element (FE) analysis is a useful tool to predict the extent of ship collision and consequent damage to structural components. However, the nonlinear dynamic analysis should be compared with experimental tests before being used for structural design. Unfortunately, experimental tests on full scale ship collision are rare and very expensive. One approach is to perform scaled collision test on typical ship structural members to validate the numerical methods for impact analysis.

Theoretical and experimental analyses of individual ship structural components under lateral impact loads, such as plates, have been widely analyzed. For example, Shen (1995) examined the dynamic plastic response of thin circular plates transversely and centrally struck by a mass with a conical head and a spherical nose. Wang et al. (1998) derived approximate formulas for the load-deflection relationship of a rigid-plastic circular plate deflected by a rigid sphere. However, it is difficult to find comparative results between experimental tests and numerical simulations on circular plates struck laterally by a mass. In most cases, the impact response is examined by penetrating the plates using quasi-static lateral loads, which does not consider the extremely high impact forces or vibrations developed at the instant of contact between the indenter and the specimen. For example, Simonsen and Lauridsen (2000) studied the mechanics of lateral indentation of a rigid sphere into a thin, ductile metal plate, including experiments, analytical theories and numerical calculations. Tabri et al. (2007) performed FE simulations on thick steel plates where the specimens were statically deformed by a spherical punch using different failure criteria. Ehlers (2010) proposed a true stress and strain relation to simulate plate punching experiments until fracture with the FE method.

The present study is a continuation of the experimental investigation reported by Sutherland and Guedes Soares (2009) on fully clamped composite, aluminium and steel circular plates subjected to lateral impact. In this paper, numerical simulations of tests on steel plates are presented in order to predict their maximum deflection, force and absorbed energy. The FE model is based on previous numerical simulations of lateral impacts on aluminium 5083/H111 circular plates (Villavicencio et al. 2010).

A brief summary of the experimental set up and the definitions adopted in the numerical model are described. Then comparisons were made between the numerical and experimental force-displacement responses for selected (low, medium and high) velocities in order both to validate and optimise the numerical simulations. Using the optimised

models from the previous step, the experimental and numerical maximum deflection and maximum force behaviours are then compared for all tested impact velocities. The deformation shape is analyzed using both shell and solid elements types and different mesh sizes, and additional comments on the stress and strain distributions, and on the energy partitioning, are then given. Finally, the behaviour of the current steel plates is compared to those of the aluminium plates studied in Villavicencio et al. (2010).

2 EXPERIMENTAL DETAILS

The experimental tests represent an impact event in which a fully clamped circular plate is struck by a mass G traveling with an initial velocity V_0 at the centre of the plate (Fig. 1). After impact, the striker G is assumed to remain in contact with the plate. Therefore, the striker and the struck point of the plate have an initial velocity V_0 at the instant of contact and a common velocity throughout the entire response. The maximum total deformation W_t is divided into two parts: maximum local indentation W_i and maximum global deflection W (Shen 1995).

The impact tests were performed using a fully instrumented Rosand IFW5 falling weight machine, which gives the variation with time of the impact force, velocity, displacement and energy of the impacted specimens. The experimental setup can be seen in Figure 2. Specimen plates

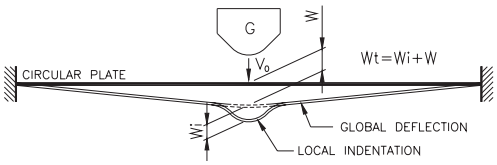

Figure 1. Clamped circular plate struck laterally at the centre by a mass.

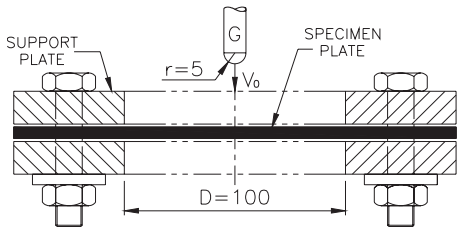

Figure 2. Experimental clamped condition.

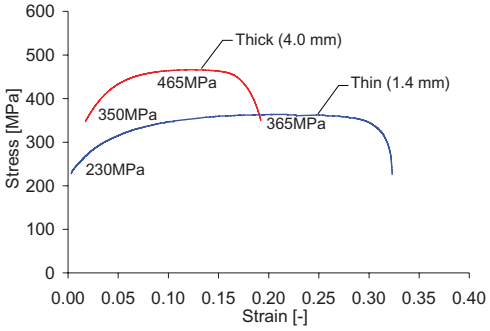

Figure 3. Engineering curves of material.

were 200 mm square and were fully clamped by four bolts between two thick 200 mm square steel plates with internal diameter 100 mm. The indenter was a hemi-spherically ended projectile of radius 5.0 mm.

In order to investigate the effects of both global deformation and local indentation, tests were carried out on steel plates for two thicknesses 1.4 and 4.0 mm (thin and thick plates respectively), using an impact mass of 3.1 and 4.9 kg respectively. Tests were carried out on virgin specimens for a range of impact velocities, from 0.5 to 6.0 m/s approximately.

The material for the thick plates is 'Structural hot rolled steel grade S235JR' whereas for the thin plates is 'Structural cold rolled steel grade ST12'. The mechanical properties of the material were obtained from tensile tests carried out on the same plates from which the impact specimens were cut. The engineering curves of both thicknesses are plotted in Figure 3. Full experimental details and discussions of the experimental results may be found in Sutherland and Guedes Soares (2009).

3 NUMERICAL MODEL

The computations were carried out using the finite element package LS-DYNA Version 971 (Hallquist 2005) which is appropriate for non-linear explicit dynamic simulations with large deformations. The FE model is based on the numerical analysis on circular aluminium plates conducted by Villavicencio et al. 2010, where a sensitivity analysis of the mesh size and the modelling of support plates to represent the experimental boundary condition were completed. In the present section the main characteristics of the FE model and improvements with respect to the previous model are summarized (Fig. 4).

The specimen plates were modelled with 4-node shell elements with 4-integration points through the

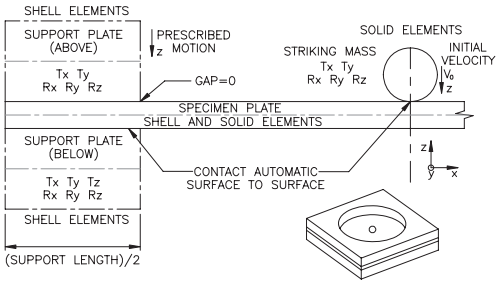

Figure 4. Details of finite element model (Villavicencio et al. 2010).

thickness (Belytshko-Lin-Tsay formulation) and with 8-node solid elements with 1-integration point (constant stress solid element formulation), both element formulations are the default in LS-DYNA. The mesh sizes of the shell elements were 2×2 and 1×1 mm for both plate thicknesses (denoted by Shell2 and Shell1 respectively). The mesh size of the solid elements was $1 \times 1 \times 1$ mm for the thick plates and $1 \times 1 \times 0.35$ mm for the thin plates (denoted by Solid1 in both cases), in order to give the same number of integration points through the thickness as in the corresponding shell models.

The support plates simulate the boundary conditions of the specimen plate, compressing the specimen as occurred in the experiments. For the striking mass only the vertical translation was free, in which direction the initial impact velocity was assigned. The indenter-specimen and support plates-specimen contact was defined as 'Automatic Surface to Surface' (Hallquist 2005).

The support plates and the striking mass were modelled as a rigid un-deformable material. 'Mat.020-Rigid' was selected from the material library of LS-DYNA and steel mechanical properties assigned. Since the falling weight was modelled as a simple sphere, an artificially large density was used to give the same mass as the one used in the experiments. To represent the specimen plate the material 'Mat.024-Piecewice linear plasticity' was selected and defined according to the exact true stress-strain curve until the onset of necking (Dieter 1986), where the true stress σ_t and the true strain ε_t are expressed in terms of the engineering stress σ_e and engineering strain ε_e (obtained from the tensile tests, and shown in Fig. 3) by:

$$\sigma_t = \sigma_e (\varepsilon_e + 1) \quad (1)$$

$$\varepsilon_t = 1n (\varepsilon_e + 1) \quad (2)$$

Since for the impact tests considered here only plastic deformation was observed, failure strain was not required for the material definition.

Strain-rate sensitivity was considered by including nominal strain-rate coefficients (Jones 1989). However, this resulted in predicting lower displacements than the experimental results and hence these strain-rate coefficients were not included in the model.

In order to try to investigate the source of vibrations seen in the experimental force-deflection results, the time interval between outputs was decreased ten times in comparison with the previous analysis on aluminium plates.

4 RESULTS AND DISCUSSION

4.1 *Force-displacement response*

Initially, in order to optimise the numerical model in terms of mesh size and element type (shell or solid), four impact velocities from the full set of experimental tests were considered. Force-displacement test results of a high, low and two intermediate velocities were compared to the numerically simulated impact responses.

For the thick plates (4.0 mm), using any of the three numerical models (Shell2, Shell1 or Solid1) gave very similar results for all four impact velocities, and in general the numerical simulations compare well with the experimental results. As an example, Figure 5 compares the experimental and numerical results for the thick plate impacted at the highest velocity of 5.9 m/s. From this figure it can be seen that, in terms of force-displacement response, the Solid1 model does not give better predictions than the computationally less demanding Shell2 or Shell1 models, although the solid models give slightly higher maximum deflection and lower maximum impact force. This was also found to be the case for the thin plates (1.4 mm).

Figures 6 and 7 compare the experimental (dashed line) and numerical (continuous line) force-displacement results for all four incident

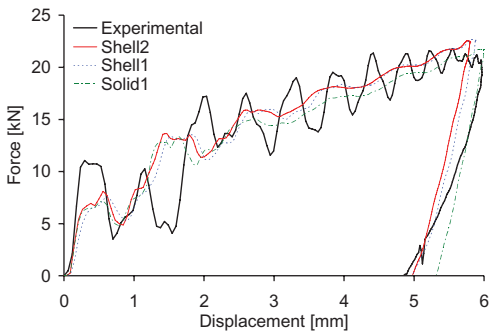

Figure 5. Force-displacement response. Thick plate (4.0 mm) impacted at 5.9 m/s.

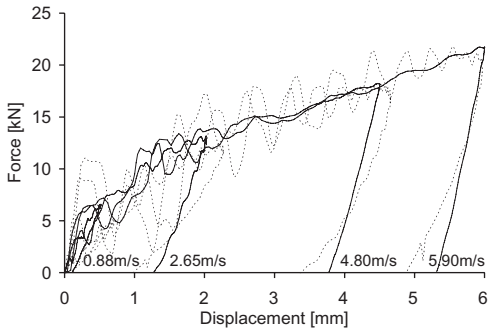

Figure 6. Force-displacement response thick steel plates. Experimental (dashed line); Numerical (continuous line).

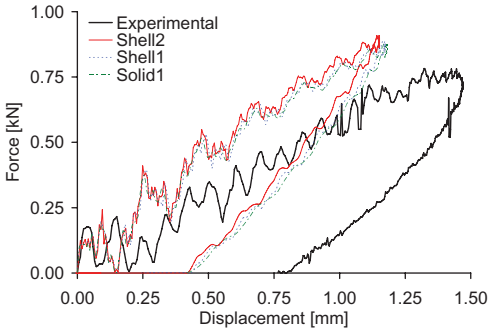

Figure 8. Force-displacement response. Thin plate (1.4 mm) impacted at 0.6 m/s.

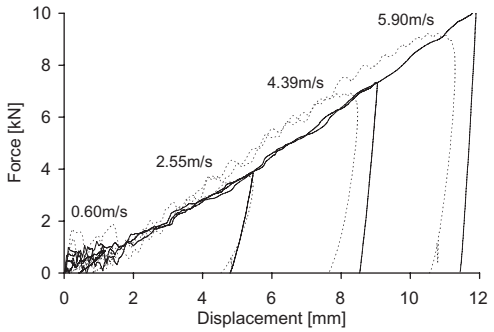

Figure 7. Force-displacement response thin steel plates. Experimental (dashed line); Numerical (continuous line).

velocities considered for the thick and thin plates respectively. Good agreement between numerical and experimental results is seen for the whole range of impact velocities, and the overlapping parts of the response for different velocities are coincident. However, for the thin plates deflection and force are slightly overestimated by the numerical model at the higher impact velocities (4.39 and 5.90 m/s). For both thin and thick plates discrepancies were seen between the experimental and numerical force-displacement responses for impacts at the lowest velocities (0.88 and 0.60 m/s respectively) as illustrated in Figure 8. These are thought to be due to experimental measurement errors which become significant when compared to the very low forces and displacements seen at these low incident energies.

All of the experimental and numerical responses in Figures 5 to 8 show oscillations during the initial stages of the impact, which are more pronounced in the experimental results, becoming more so as the severity of the impact test was increased. These vibrations are also more apparent for the thick than for the thin plates. However, since the oscillations are harmonic and sufficient cycles occur prior to the end of the test the energy values are sufficiently accurate. The source of this vibratory response could be due to two possible phenomena:

i. Due to the inertia of the plate, at the initiation of contact the impact mass and plate vibrate around the contact stiffness as the plate begins to move.
ii. Since in the experiments the impact mass is not a sphere, but a hemispherical-ended bar connected via a load cell to a large mass, vibrations may be set up in this (and/or other) part(s) of the impact machine.

Phenomena (i) would be apparent in both experimental and numerical responses. However, phenomena (ii) would only be apparent in the experimental response.

The fact that vibrations of the same frequency were noted in the experimental force measurements after separation of the impact mass and plate at the end of the impact event suggest that vibrations in the test machine (ii) were present in the experimental results. Also, the presence of (less severe) vibrations in the numerical results suggest that oscillations due to the contact stiffness-plate inertia phenomena (i) are also present in the experimental results, hence the larger vibrations seen experimentally.

Since only oscillations due to (i) are valid material impact responses, it would be pertinent to filter out any experimental oscillations due to machine vibrations. However, in practice this filtering may well affect the impact response of interest, and it is extremely difficult to ensure that only the machine vibrations are filtered out. These results show that the filtering and interpretation of impact test results is by no means a straightforward, clear-cut process.

Since no significant increase in accuracy was seen in the results described above through using

the finer meshed Shell1, or the Solid1 models, the less computationally expensive Shell2 model was then used to calculate the maximum transversal deflection and impact force for the full range of impact velocities carried out in the experiments.

Figures 9 and 10 show these experimental-numerical comparisons. Excellent agreement for all incident velocities is shown in Figure 9 between the numerical and experimental maximum deflection results for thick plates. Figure 9 shows that the experimental maximum deflection is also very well predicted by the numerical analyses for thin plates at lower impact velocities. However, the experimental thin plate values of maximum deflection and maximum force in Figures 9 and 10 respectively become slightly lower than their numerical counterparts when the impact velocities exceed 3.0 m/s. This is seen to be due to the slightly different shapes of the force-deflection responses of Figure 7, where the experimental curves at higher velocities exhibit slightly higher stiffness, but the drop of force to zero at the end of the impact event occurs at a lower deflection than for the numerical response. In fact, when the experimental and numerical energy values (obtained by integration of the relevant force-displacement curves) are compared the numerical results underestimate the amount of impact energy irreversibly absorbed by the plates by an average of 12% of the incident energy.

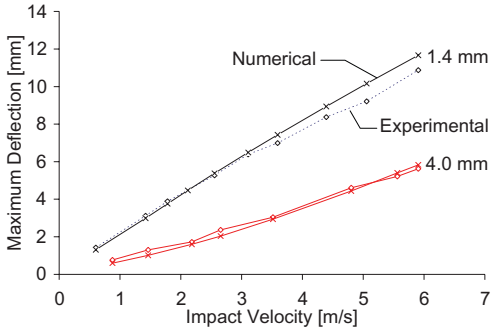

Figure 9. Maximum deflection-velocity. Thick and thin plates.

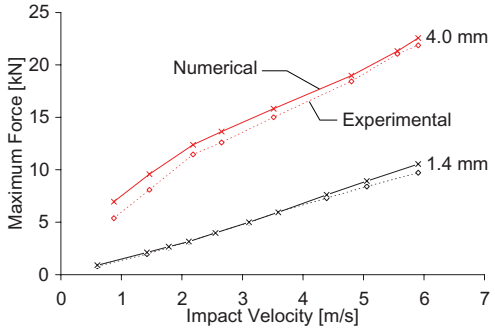

Figure 10. Maximum force-velocity. Thick and thin plates.

It is not clear exactly what causes these discrepancies, but it appears that mechanism(s) of energy absorption seen in reality are not modelled correctly in the numerical analyses, for example the dissipation of heat generated during plastic deformation. It is also possible that this slightly higher stiffer response is due to strain-rate effects that were not included in the FEA.

Since the numerical model is very sensitive to the true stress-strain curve, any slight errors in this input could explain discrepancies between numerical and experimental results. However, since this behaviour was obtained through in-house tensile tests cut from the same sheets from which the impacted plates were cut, confidence in this curve is high.

Despite generally good agreement, the thick plate experimental maximum forces are over-predicted by the numerical model, especially at velocities lower than 2.5 m/s, at which point an inflection is seen in both the experimental and numerical curves. This inflection could be due to a change from the mainly contact-indentation dominated damage seen at lower velocities to global plate plastic deformations at higher velocities. It is suggested that this over-prediction of the experimental impact force could be due to the way in which the local contact is modelled numerically, since this would only become significant in impacts where contact damage is dominant, as is the case for the thick plates at lower incident velocities. This could be because the striking mass was modelled as a rigid body, when in fact deformation at the impactor nose could have occurred experimentally.

4.2 *Plastic deformation, maximum stresses and energy partition*

Once the force-displacement response was validated against the experimental results, the numerical simulations were then used to give information concerning the specimen plastic deformation, the maximum stresses, and the partition of the impact energy.

It is beneficial to be able to predict the shape of the deformation due to both global deflection and local indentation. Local indentation is divided in two parts: local out-of-plane plate deformation (where the plate wraps around the indenter), and the indentation of the mass into the plate thickness. For the thick plates the Solid1 model gives a better definition of the shape of the deformation than does the Shell2 or Shell1 model, because only solid elements are able to model the change in plate

thickness associated with the indentation of the mass into the plate at the impact point, which is significant for the thick plates (Fig. 11a). For the thin plates indentation is more significant in terms of out-of-plane plate deformation, (Fig. 11b) and hence the only requirement is a fine shell mesh for accurate modelling of the local indentation of the thin plates. A fine mesh is also the only requirement for the accurate modelling of the global plate deformation of both thin and thick plates.

In Villavicencio et al. (2010) the maximum stress for impacted aluminium plates was found to occur on the surface opposite to the impact point for both shell and solid models, but that near the support the stresses did not differ between upper and lower faces. The numerical models of the current steel plates also show that the maximum plastic strain occurs on the lower surface opposite to the impact point, and indicate the presence of plastic strain throughout the plate thickness at high impact velocities. However, at lower impact energies, elements near the neutral axis did not undergo plastic strain.

Effective stresses were also observed to decrease gradually from the impact point to the supports. Figure 12 shows the maximum von Mises stress distribution on the plate lower surface when impacted at the highest velocity. For the thick plates only that part of the specimen within the annular cut-out in the support plates is affected by the impact. However, for the thin plates the stresses in the clamped area of the specimen are also seen to be affected by the impact. This is thought to be mainly due to the slippage of the specimen plate between the support plates due to the higher deflections and hence membrane forces experienced by the thin plates.

Temporal variations in the energy during the impact system are shown in Figure 13. The kinetic energy of the falling mass is dissipated

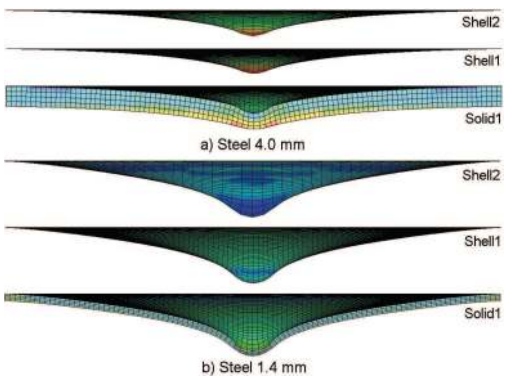

Figure 11. Shape of the deformation. Impact velocity 5.9 m/s.

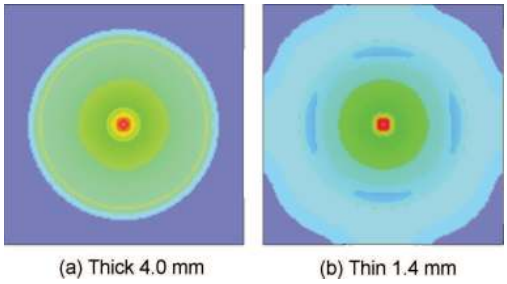

Figure 12. Maximum von Mises stress distribution. Impact velocity 5.9 m/s.

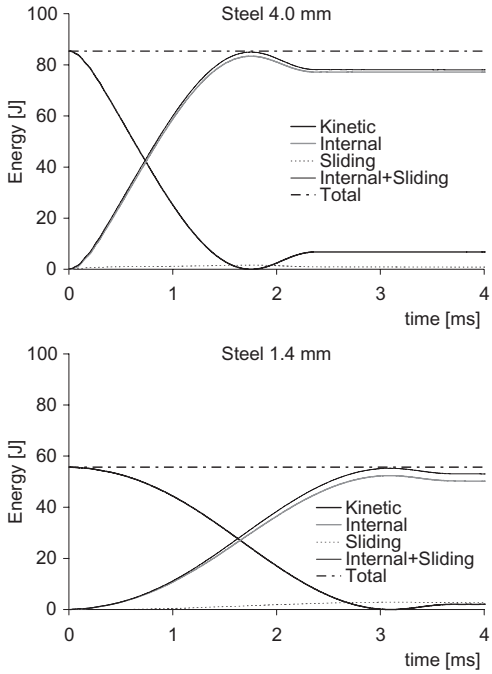

Figure 13. Energy partitioning. Impact velocity 5.9 m/s.

as a combination of internal and sliding energies (the hourglass energy was zero in the numerical simulations). The internal energy consists of elastic strain energy and plastically dissipated energy. The sliding energy (or contact energy) is due to the friction included in the support plates-specimen contact definition. During the initial instants of the impact event the internal energy is due to elastic deformation only, and is almost entirely responsible for the dissipation of kinetic energy as the sliding energy is extremely small. However, as the impact progresses both plastic deformation energy becomes significant and sliding energy increases. Although the latter remains a very small contribution to the total energy conversion in all cases,

the proportion of sliding energy is slightly higher for the thin plates due to the small radial displacements between the support plates (slippage) experienced by these specimens (Fig. 12).

4.3 *Comparisons with aluminium impact response*

The impact tests on the present steel plates were part of a wider experimental study by Sutherland and Guedes Soares (2009), which also considered the aluminium plates numerically simulated in Villavicencio et al. (2010). Since impact response is a structural and not a material property, the plate thicknesses of the different materials were chosen to give plate bending equivalence so that valid comparisons between the different materials were possible. Hence, the thicknesses of the aluminium plates were 6.0 and 2.0 mm (thick and thin respectively). Here, the experimental and numerical impact responses of the steel and aluminium plates are compared.

The improvements included in the FE model of the steel plates have been retrospectively considered in the aluminium FE model, and the numerical results of the latter updated accordingly. In the new aluminium models, the shell elements have 6 and 4 integration points for the 6.0 and 2.0 mm thick plates, respectively. The thin plate solid model used 4 elements through the thickness instead of the 2 defined in the previous model. However, for the thick plates the through-thickness number of elements of the solid model was maintained at 6. These modifications were included in order to define the same number of integration points through the thickness for both shell and solid models. The time interval between outputs was also decreased ten-fold.

The modified aluminium numerical models were again initially evaluated and optimised in terms of element type, using the maximum and minimum experimental impact velocities for each plate thickness in this case. However, it was assumed that, as found previously for the aluminium plates in Villavicencio et al. (2010), and for the steel plate impacts of this paper, mesh size was not significant and hence only the Solid1 and Shell2 elements were considered. As for the steel plates, the aluminium shell and solid models give very similar force-displacement results, and good agreement with the experimental results is seen. As an example, Figure 14 gives a comparison of the experimental and numerical results for a thin aluminium plate impacted at 5.9 m/s.

For both thicknesses, the improvements to the aluminium numerical model gave better agreement between the shell and solid models, which has been illustrated by the inclusion of the 'old' Shell2 model results in Figure 14. Very

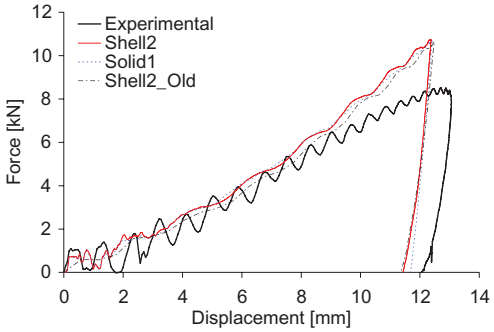

Figure 14. Force-displacement response thin aluminium plate. Impact velocity 5.9 m/s.

similar discrepancies between the numerical and experimental force-deflection responses were seen for the aluminium plates at the very lowest incident velocities as were seen for the steel specimens (Fig. 8). Again, these are thought to be due to the relatively high significance of experimental errors when compared to the very small force and displacement measurements that must be made for these very low-energy impact events.

As for the steel plates, since there was seen to be no advantage in using the more computationally expensive solid elements, the Shell2 model was selected to calculate the maximum deflections and forces for all experimental impact velocities, as shown in Figures 15 and 16. These plots show very good, and similar, agreement between experimental and numerical results as seen for the steel plates in Figures 9 and 10. However, the agreement between experimental and numerical maximum deflection for the thin aluminium plates seen in Figure 15 continues up to the highest impact velocities (as opposed to the numerical overestimation of maximum deflection at high impact energies for the steel plates seen in Fig. 9), although the experimental curve does also dip at higher velocities. The slight overestimation of maximum force for thin steel plates at higher velocities (Fig. 10) is also seen in Figure 16 for the aluminium tests, and again more impact energy is irreversibly absorbed experimentally than numerically predicted.

The overestimation of maximum impact force by the numerical model seen for thick steel plates (Fig. 10) is seen to be even more significant in Figure 16 for the thick aluminium plates. Again, it is thought that this is due to the way in which the local impactor-plate contact/indentation is modelled. The inflection observed in the force-velocity curve of the thick steel plates at around 2.5 m/s, thought to be due to the initiation of significant global plastic deformation, is also seen in that of the thick aluminium plates.

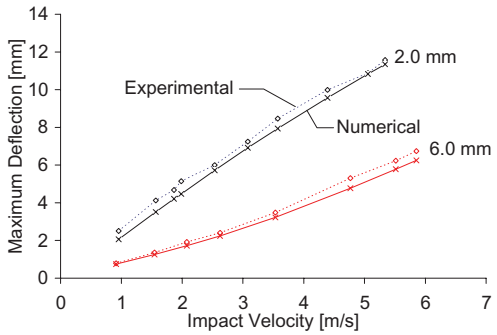

Figure 15. Maximum deflection-velocity.

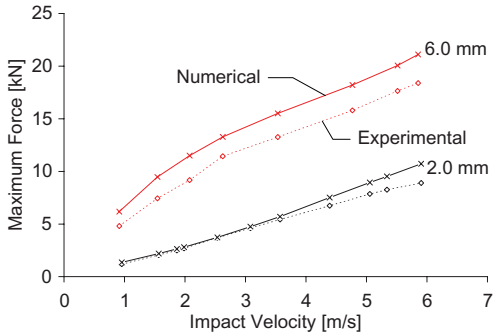

Figure 16. Maximum force-velocity.

5 CONCLUSIONS

Detailed information of the impact response of clamped steel and aluminium circular plates has been obtained through non-linear explicit dynamic simulations using the LS-DYNA software package. The results obtained were in good agreement with those of previous experimental tests, indicating that relatively coarse meshes using shell elements are sufficient to predict the maximum deflections and forces for the entire plastic response of both steel and aluminium.

The support plates representing the experimental boundary conditions were capable of representing some small longitudinal displacement of the specimen plate between the supports, especially for the thin plates at higher velocities.

The numerical simulations gave a good understanding of the shape of the deformation in plates subjected to impact loads. In terms of indentation, a fine meshed solid model gave a better definition of the shape of the deformation since this was able to model both the deformation around the indenter and also the change in plate thickness at the impact point. The maximum plastic strain occurred on the lower surface of the plate, and the presence of plastic strain throughout the plate thickness at high impact velocities was seen. However, at lower impact energies elements near the neutral axis were not predicted to undergo plastic strain.

Although generally very good agreement was obtained, two discrepancies between numerical and experimental were observed, that were very similar for both steel and aluminium impacts:

i. For thin plates at higher velocities, numerical predictions overestimated the experimental maximum forces, and underestimated the energy irreversibly absorbed. The numerical simulations also overestimated the thin steel plate maximum experimental deflection for higher velocity impacts. A slightly stiffer response was also seen experimentally. It is postulated that this could be due to more slippage, more plastic deformation generated heat dissipation, or strain-rate dependant effects, or a combination of these effects.
ii. For thick plates the maximum forces seen experimentally were overestimated by the numerical model. It is thought that this is due to the way in which the impactor-plate local contact, and plate-support contact has been modelled.

Further work would be beneficial to refine the model in terms of the static coefficients of friction used, the modelling of the striking mass, possible material property strain-rate effects, and additional energy absorption mechanisms. Since it is highly probable that more than one of these phenomena could be influential, and more importantly that there may well be interactions between these effects, any further work must be carefully designed to give a numerical model optimised in terms of all such effects.

The investigation of the impact of thicker plates would also be worthwhile. These could be geometrically scaled-up versions of the present plates, or thicker plates of similar size to the present ones. In the former case, a dimensional analysis approach to develop scaling laws, such as used with success in Sutherland and Guedes Soares (2007) for laminated glass-polyester plates, could be used. This would also identify any unexpected scaling model shortcomings, or 'size effects' that could lead to inaccurate prediction of full-scale in-service behaviour from laboratory scale tests.

For the latter case of plates of lower length to thickness ratio, a far more contact/indentation dominated behaviour, with little global plate deformation or influence of boundary conditions, would be expected. Hence, the use of refined solid element models would be necessary to represent the indentation into the plate thickness. The study of lower length to thickness ratio plates could also be used to approximate the behaviour expected for thinner plates at, or near to, stiffeners.

ACKNOWLEDGMENTS

The work has been performed in the scope of the project MARSTRUCT, Network of Excellence on Marine Structures (http://www.mar.ist.utl.pt/marstruct/), which has been financed by the EU through the GROWTH Programme under contract TNE3-CT-2003-506141.

The first author has been financed by the Portuguese Foundation for Science and Technology, under contract SFRH/BD/46369/2008.

REFERENCES

Dieter GE. 1986. Mechanical behavior under tensile and compressive loads. ASM Handbook. 8: 99–10.

Ehlers S. 2010. Strain and stress relation relation until fracture for finite element simulations of a thin circular plate. Thin-Walled Structures. 48 (1): 1–8.

Hallquist JO. 2005. LS-DYNA Theory Manual. Livermore Software Technology Corporation.

Jones N. 1989. Structural Impact. Cambridge University Press.

Shen WQ. 1995. Dynamic plastic response of thin circular plates struck transversely by nonblunt masses. Int. J. Solids Structures. 32 (14): 2009–2021.

Simonsen BC, Lauridsen LP. 2000. Energy absorption and ductile failure in metal sheets under lateral indentation by a sphere. International Journal of Impact Engineering. 24 (10): 1017–1039.

Sutherland LS, Guedes Soares C. 2007. Scaling of impact on low fibre-volume glass–polyester laminates. Composites: Part A. 38: 307–317.

Sutherland LS, Guedes Soares C. 2009. Impact behaviour of GRP, aluminium and steel plates. Analysis and Design of Marine Structures; Guedes Soares & Das (eds). Taylor & Francis Group: London. 293–300.

Tabri K, Alsos H, Broekhuijsen J, Ehlers S. 2007. A benchmark study on ductile failure criteria for shell elements in multiaxial stress state. Advancements in Marine Structures, Guedes Soares & Das (eds). Taylor & Francis Group: London. 401–409.

Villavicencio R, Sutherland LS, Guedes Soares C. 2010. Numerical simulation of transversely impacted, clamped circular aluminium plates. 5th International Conference on Collision and Grounding of Ships; Espoo, Finland. 104–112.

Wang G, Ohtsubo H, Arita K. 1998. Large deflection of a rigid-plastic circular plate pressed by a sphere. Journal of Applied Mechanics. 65 (2): 533–535.